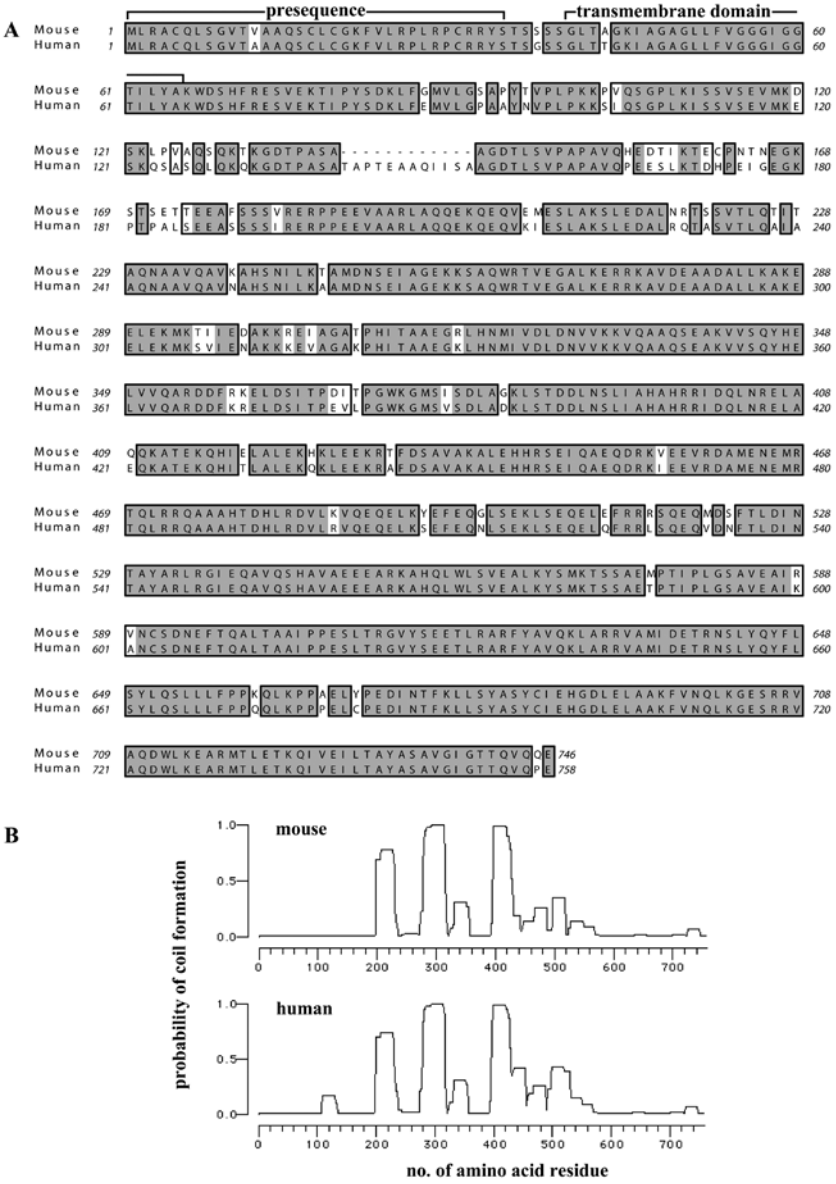
A
presequence
transmembrane domain
Mouse 1 MLRACQLSGVTVAAQSCLCGKFVLRPLRPCRRYSTSSSSGLTAGKIAGAGLLFVGGGIGG 60
Human 1 MLRACQLSGVTAAAQSCLCGKFVLRPLRPCRRYSTSGSSGLTTGKIAGAGLLFVGGGIGG 60
Mouse 61 TILYAKWDSHFRESVEKTIPYSDKLFGMVLGSAPYTVPLPKKPVQSGPLKISSVSEVMKD 120
Human 61 TILYAKWDSHFRESVEKTIPYSDKLFEMVLGPAAYNVPLPKKSIQSGPLKISSVSEVMKE 120
Mouse 121 SKLPVAQSQKTKGDTPASA----------AGDTLSVPAPAVQHEDTIKTECPNTNEGK 168
Human 121 SKQSASQLQKQKGDTPASATAPTEAAQIISAAGDTLSVPAPAVQPEESLKTDHPEIGEGK 180
Mouse 169 STSETTEEAFSSSVRERPPEEVAARLAQQEKQEQVEMESLAKSLEDALNRTSSVTLQTTT 228
Human 181 PTPALSEEASSSSIRERPPEEVAARLAQQEKQEQVKIESLAKSLEDALRQTASVTLQALA 240
Mouse 229 AQNAAVQAVKAHSNILKTAMDNSEIAGEKKSAQWRTVEGALKERRKAVDEAADALLKAKE 288
Human 241 AQNAAVQAVNAHSNILKAAMDNSEIAGEKKSAQWRTVEGALKERRKAVDEAADALLKAKE 300
Mouse 289 ELEKMKTIIEDAKKREIAGATPHITAAEGRLHNMIVDLDNVVKKVQAAQSEAKVVSQYHE 348
Human 301 ELEKMKSVIENAKKKEVAGAKPHITAAEGKLHNMIVDLDNVVKKVQAAQSEAKVVSQYHE 360
Mouse 349 LVVQARDDFRKELDSITPDITPGWKGMSISDLAGKLSTDDLNSLIAHAHRRIDQLNRELA 408
Human 361 LVVQARDDFKRELDSITPEVLPGWKGMSVSDLADKLSTDDLNSLIAHAHRRIDQLNRELA 420
Mouse 409 QQKATEKQHIELALEKHKLEEKRTFDSAVAKALEHHRSEIQAEQDRKVEEVRDAMENEMR 468
Human 421 EQKATEKQHITLALEKQKLEEKRIAFDSAVAKALEHHRSEIQAEQDRKIEEVRDAMENEMR 480
Mouse 469 TQLRRQAAAHTDHLRDVLKVQEQELKYEFEQGLSEKLSEQELEFRRRSQEQMDSFTLDIN 528
Human 481 TQLRRQAAAHTDHLRDVLRVQEQELKSEFEQNLSEKLSEQELQFRRLSQEQVDNFTLDIN 540
Mouse 529 TAYARLRGIEQAVQSHAVAEEEARKAHQLWLSVEALKYSMKTSSAEMPTIPLGSAVEAIR 588
Human 541 TAYARLRGIEQAVQSHAVAEEEARKAHQLWLSVEALKYSMKTSSAETPTIPLGSAVEAIK 600
Mouse 589 VNCSDNEFTQALTAAIPPESLTRGVYSEETLRARFYAVQKLARRVAMIDETRNSLYQYFL 648
Human 601 ANCSDNEFTQALTAAIPPESLTRGVYSEETLRARFYAVQKLARRVAMIDETRNSLYQYFL 660
Mouse 649 SYLQSLLLFPPKQLKPPAELYPEDINTFKLLSYASYCIEHGDLELAAKFVNQLKGESRRV 708
Human 661 SYLQSLLLFPPQQLKPPPELCPEDINTFKLLSYASYCIEHGDLELAAKFVNQLKGESRRV 720
Mouse 709 AQDWLKEARMTLETKQIVEILTAYASAVGIGTTQVQQE 746
Human 721 AQDWLKEARMTLETKQIVEILTAYASAVGIGTTQVQPE 758
B
mouse
human
probability of coil formation
1.0
0.5
0.0
0
100
200
300
400
500
600
700
no. of amino acid residue

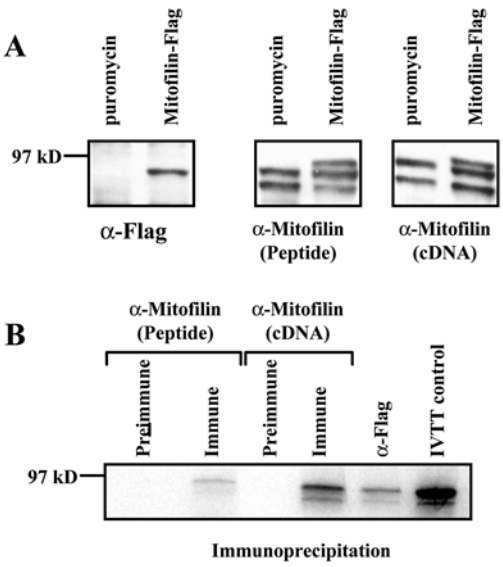
A
puromycin
Mitofilin-Flag
puromycin
Mitofilin-Flag
puromycin
Mitofilin-Flag
97 kD
α-Flag
α-Mitofilin
(Peptide)
α-Mitofilin
(cDNA)
B
α-Mitofilin
(Peptide)
α-Mitofilin
(cDNA)
Preimmune
Immune
Preimmune
Immune
α-Flag
IVTT control
97 kD
Immunoprecipitation

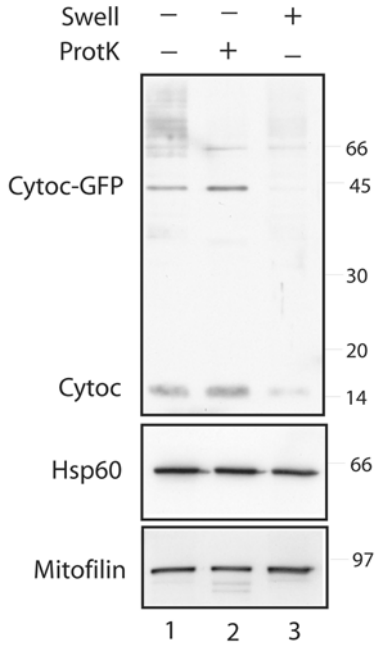
Swell – – +
ProtK – + –
Cytoc-GFP
Cytoc
Hsp60
Mitofilin
66
45
30
20
14
66
97
1 2 3

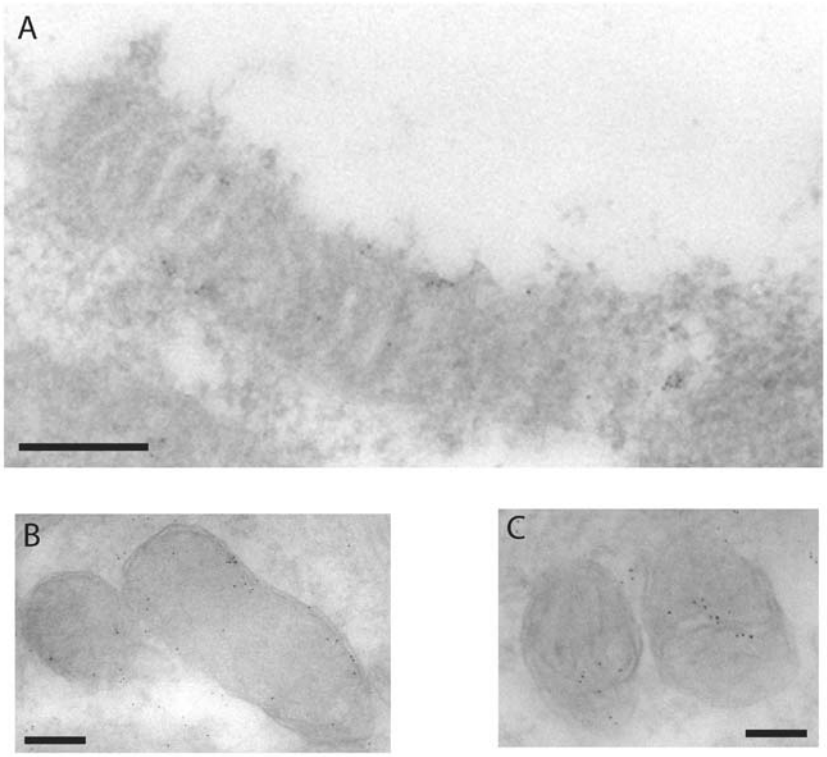
A
B
C
D
100
75
50
25
0
% Gold Particles
Cristae
Rim
Cristae
Rim
Cristae
Rim
Porin
F1 ATPase
Mitofilin

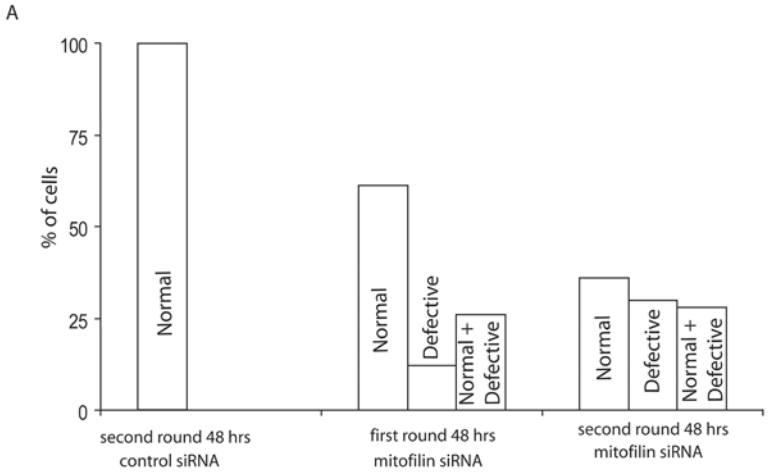
A
100
75
50
25
0
% of cells
Normal
Normal
Defective
Normal + Defective
Normal
Defective
Normal + Defective
second round 48 hrs
control siRNA
first round 48 hrs
mitofilin siRNA
second round 48 hrs
mitofilin siRNA

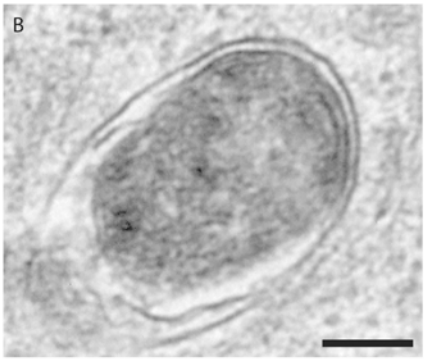
B

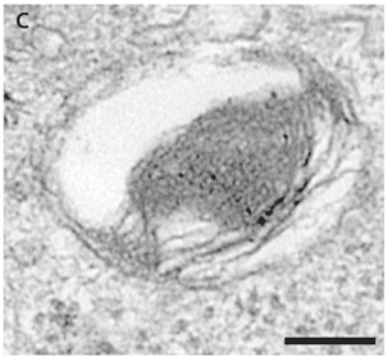
C

Online Supplemental Material

Results

Generation and characterization of anti-mitofilin antibodies

To study the role of *mitofilin* in mouse, we cloned a murine *mitofilin* cDNA by PCR from an embryonic day 17 cDNA library (Clontech) using primer sequences derived from mouse EST database. The relevant nucleotide sequence has been deposited at GenBank (Accession No. AK049189). Mouse mitofilin encodes a 747-amino acid protein with a predicted molecular weight of 89 kD, and shows 88% sequence identity and 92% sequence similarity to human mitofilin (Figure S1). We then generated two polyclonal antibodies (Abs) against mouse mitofilin, one of which was raised against amino acid residues 123-135 and 162-174 of mouse mitofilin, the other against the full-length protein. Western blot analysis using either Ab revealed Flag-tagged and endogenous mitofilin in mitofilin-Flag transfected C2C12 cells (Figure S2A). Endogenous mouse mitofilin, like human mitofilin, existed as a doublet of slightly different sizes. The pre-immune sera for both Abs failed to stain mitofilin (Unpublished data). Both Abs, but not the pre-immune sera, precipitated in vitro translated and radiolabeled mitofilin (Figure S2B).

Subcellular fractionation of HeLa cells expressing cytochrome c-GFP

To exclude the possibility that the GFP fusion protein may affect the submitochondrial localization of cytochrome c, mitochondria were isolated from HeLa cells expressing cytochrome c-GFP and subjected to swelling or proteinase K treatment (Figure S3). Treatment of mitochondria with proteinase K without swelling did not affect cytochrome c-GFP, whereas swelling resulted in loss of the protein as in the case of the endogenous cytochrome c, indicating its localization to the intermembrane space. Hsp60, a soluble matrix protein, and mitofilin were not affected by the exogenous protease treatment without swelling or swelling alone, indicating that the inner membrane and its associating proteins were intact.

Legends to figures

Figure S1. Mitofilin is a mitochondrial protein with a predicted transmembrane segment and coiled coil domains. Comparison of the predicted amino acid sequences of mouse

and human mitofilin. (A) Amino acid sequences of mouse and human mitofilin were aligned using Macvector. Identical amino acids are indicated in shaded boxes and similarities as empty boxes. The predicted cleavable presequence (Gavel and von Heijne, 1990) and transmembrane segment (Krogh *et al.*, 2001) is indicated. (B) Coiled coil prediction (Lupas *et al.*, 1991) for the mouse and human mitofilin protein sequences. The window size used was 21.

Figure S2. Characterization of anti-mitofilin antibodies. (A) Western blot analysis of mitofilin. C2C12 myoblasts stably expressing mitofilin-Flag and $Puro^r$ were used to prepare cellular lysate that were size-fractionated by SDS-PAGE and probed with α-Flag, α-mitofilin (peptide) and α-mitofilin (cDNA) antibodies (A). The antibodies were also tested for immunoprecipitation of in vitro transcribed and translated (IVTT) mitofilin-Flag (B). The preimmune sera were used as controls. The immunoprecipitates were size-fractioned by SDS-PAGE, and the gel exposed for autoradiography.

Figure S3. Submitochondrial localization of cytochrome c-GFP. Mitochondria isolated from the cytochrome c-GFP expressing HeLa cells were treated with proteinase K or swelled, separated on SDS-PAGE and analyzed by Western blotting with α-cytochrome c, α-Hsp60 and α-mitofilin (cDNA) Abs. The molecular weight markers (kD, Amersham Biosciences) are indicated.

Figure S4. Immunolabeling of mitochondria in mouse embryonic heart. (A) Ultrathin section of the 15.5 day old rat embryonic heart mitochondria stained with α–mitofilin (cDNA), porin (B) and F1 ATPase (C) showing outer rim and internal crisate staining. 5nm gold conjugated secondary antibody. Size bar 250nm. (D) Quantitation of the immunogold particles staining either the rim or cristae following detection with antibody against porin, F1 ATpase and mitofilin. The data is presented as an average of mitochondrial staining counted from 15 independent cells.

Figure S5. Quantitation of defective mitochondria in mitofilin siRNA treated cells. (A) A total of 60 (control siRNA), 57 and 50 (mitofilin siRNA) independent cells following 48

hrs of first and second round of siRNA were observed to detect defective mitochondria. Electron micrscopic image of an early (B) and late (C) autophagic mitochondria. Images were obtained from cells treated with mitofilin siRNA 48 hrs after two rounds. Size bar 250 nm.

References

Gavel, Y., and von Heijne, G. (1990). Cleavage-site motifs in mitochondrial targeting peptides. Protein Eng *4*, 33-37.
Krogh, A., Larsson, B., von Heijne, G., and Sonnhammer, E.L. (2001). Predicting transmembrane protein topology with a hidden Markov model: application to complete genomes. J Mol Biol *305*, 567-580.
Lupas, A., Van Dyke, M., and Stock, J. (1991). Predicting coiled coils from protein sequences. Science *252*, 1162-1164.